J Arid Land (2014) 6(6): 647–655
doi: 10.1007/s40333-014-0066-9
jal.xjegi.com; www.springer.com/40333

Evaluation of an erosion-sediment transport model for a hillslope using laboratory flume data

Anya Catherine C ARGUELLES[1], MinJae JUNG[2], Kristine Joy B MALLARI[2], GiJung PAK[1], Hafzullah AKSOY[3], Levent M KAVVAS[4], Ebru ERIS[5], JaeYoung YOON[1,2*], YoungJoon LEE[6], SeonHwa HONG[6]

[1] Department of Environmental Engineering, Korea University, Sejong 339-700, Korea;
[2] Program in Environmental Technology and Policy, Korea University, Sejong 339-700, Korea;
[3] Department of Civil Engineering, Istanbul Technical University, Maslak 34469, Istanbul, Turkey;
[4] Department of Civil and Environmental Engineering, University of California, Davis, California 95616, USA;
[5] Department of Civil Engineering, Ege University, Bornova 35100, Izmir, Turkey;
[6] Geum-River Environment Research Center, National Institute of Environmental Research, Okcheon, Chungbuk 373-804, Korea

Abstract: Climate change can escalate rainfall intensity and cause further increase in sediment transport in arid lands which in turn can adversely affect water quality. Hence, there is a strong need to predict the fate of sediments in order to provide measures for sound erosion control and water quality management. The presence of micro-topography on hillslopes influences processes of runoff generation and erosion, which should be taken into account to achieve more accurate modelling results. This study presents a physically based mathematical model for erosion and sediment transport coupled to one-dimensional overland flow equations that simulate rainfall-runoff generation on the rill and interrill areas of a bare hillslope. Modelling effort at such a fine resolution considering the flow connection between interrill areas and rills is rarely verified. The developed model was applied on a set of data gathered from an experimental setup where a 650 cm×136 cm erosion flume was pre-formed with a longitudinal rill and interrill having a plane geometry and was equipped with a rainfall simulator that reproduces natural rainfall characteristics. The flume can be given both longitudinal and lateral slope directions. For calibration and validation, the model was applied on the experimental results obtained from the setup of the flume having 5% lateral and 10% longitudinal slope directions under rainfall intensities of 105 and 45 mm/h, respectively. Calibration showed that the model was able to produce good results based on the R^2 (0.84) and NSE (0.80) values. The model performance was further tested through validation which also produced good statistics (R^2=0.83, NSE=0.72). Results in terms of the sedigraphs, cumulative mass curves and performance statistics suggest that the model can be a useful and an important step towards verifying and improving mathematical models of erosion and sediment transport.

Keywords: climate change; erosion; rill and interrill; physically based model; sediment transport

Citation: Anya Catherine C ARGUELLES, MinJae JUNG, Kristine Joy B MALLARI, GiJung PAK, Hafzullah AKSOY, Levent M KAVVAS, Ebru ERIS, JaeYoung YOON, YoungJoon LEE, SeonHwa HONG. 2014. Evaluation of an erosion-sediment transport model for a hillslope using laboratory flume data. Journal of Arid Land, 6(6): 647–655. doi: 10.1007/s40333-014-0066-9

Growing concerns about climate change are considered as an important dimension for environmental planning. Increase in rainfall intensity is projected to be one of the notable consequences of climate change and possibly results in the anticipated acceleration of hydrological cycles (Shaw et al., 2005; Hirabayashi et al., 2008; Mailhot and Duchesne, 2010). Soil erosion is expected to increase with higher rainfall intensity due to higher detachability rate, making arid lands more vulnerable.

On the other hand, drought, being the other consequence of climate change, together with strengthened human activities affects lake level and area (Ma et al., 2011). Lake areas and reservoir capacities shrink

*Corresponding author: Jaeyoung YOON (E-mail: jyyoon@korea.ac.kr)
Received 2013-03-24; revised 2014-01-27; accepted 2014-03-03

due to further sediment deposition. In arid regions, seasonal or annual drought cycles cause soils to suffer extensive erosion (Sharaiha and Ziadat, 2007). Soils, particularly in barren lands which are more vulnerable to erosion, are easily deposited into rivers and seas during heavy downpour.

It is very clear from the above statements that climate change is strongly related to erosion and sediment transport. Hence, the research on erosion-sediment transport models is critical for sound erosion control and water quality management.

In modeling hillslope processes, the influence of microtopography on overland flow and erosion and sediment transport is of great importance. The upland consists of rills and interrill areas. Rills are small rivulets on hillslopes where runoff is concentrated while the areas between the rills are the interrill areas (Toy et al., 2002). It is understood that rills contain greater flow and sediment discharges compared to the interrill areas.

Extensive literature is available on the modelling of erosion and sediment transport. Models that have been developed can be categorized as being lumped or distributed and conceptual, empirical or physically based. A physically based model, which this study focuses on, uses mass conservation equations of sediment. Examples of physically based erosion-sediment transport models are KINEROS (Smith, 1981), WESP (Lopes, 1987), SEM (Storm et al., 1987), SHESED (Wicks, 1988; Wicks and Bathurst, 1996) and EUROSEM (Morgan et al., 1998). Though useful in physically describing the processes at a watershed scale, local features such as rills and interrills that can be important at a hillslope scale are not modeled explicitly in these models.

This paper presents a physically based erosion-sediment transport model presented by Aksoy and Kavvas (2001) coupled to one-dimensional (1-D) overland flow models developed for rill and interrill areas by Arguelles et al. (2013). Modelling effort at such a fine spatial resolution considering the flow connection between interrill areas and rills is rarely verified due to difficulty involved with simulated rainfall experiments. There have been few studies of models related to erosion and sediment transport tested in laboratory setups of bare hillslopes (Liu et al., 2006; Deng et al., 2008; An and Liu, 2009). Among these, Deng et al. (2008) did not recognize rill and interrill in their governing equations while Liu et al. (2006) recognized these microtopographical features but still used a single governing equation (1-D) to describe the sediment dynamics. An and Liu (2009) tried to overcome this shortcoming by writing separate governing equations for interrill (2-D) and rill (1-D), though connection between them had to be addressed by an ad hoc relationship. In addition, calibrations were only attempted in these studies for two (Liu et al., 2006; An and Liu, 2009) or three (Deng et al., 2008) runs, and no verification was done. The objective of this paper is to calibrate and verify the model based on simpler 1-D governing equation for interrill that accounts for dynamic connection with rill using the experimental data collected from a laboratory set-up of a bare hillslope (Aksoy et al., 2012).

1 Materials and methods

1.1 Experimental setup

Overland flow and sediment discharge from the rill and interrill areas were taken from the experiment designed and performed by researchers at Istanbul Technical University (Aksoy et al., 2012). Figure 1 describes the experimental setup as a 6.50 m×1.36 m erosion flume with a depth of 17 cm. The slope of the flume can be adjusted along the longitudinal and lateral directions. It was equipped with four or five Vee-Jet nozzles spaced at 125–145 cm depending on the rainfall intensity to serve as the rainfall simulator over the flume. The rainfall granulometry analysis showed that the raindrop sizes were from 2.19–3.13 (φ values) in terms of mean diameter (D_{50}) and were within the range found in the literature available regarding characteristics of natural rainfall. The velocity when the raindrops hit the soil in the flume is called impact velocity. How close the impact velocity is to the terminal velocity is important in rainfall simulation studies for ensuring the natural rainfall characteristics. It was seen that the impact velocities approach terminal velocities within a range of relative error from 5.7% to 15.4%.

In Fig. 2, it shows that most of the interrill area contributes flow to the rill and the flow from the rest small

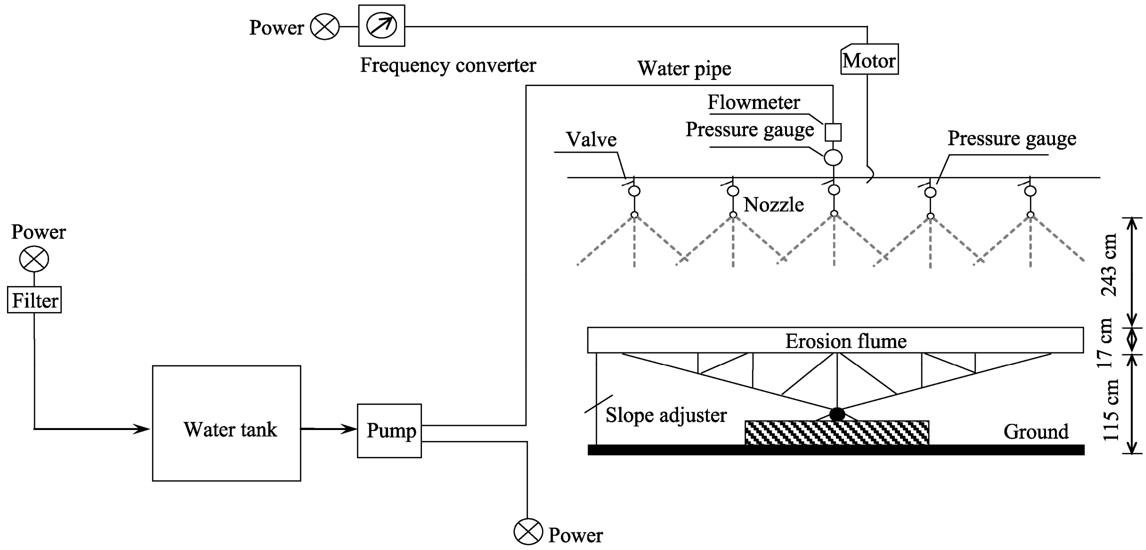

Fig. 1 Sketch of the rainfall simulator and erosion flume (Aksoy et al., 2012)

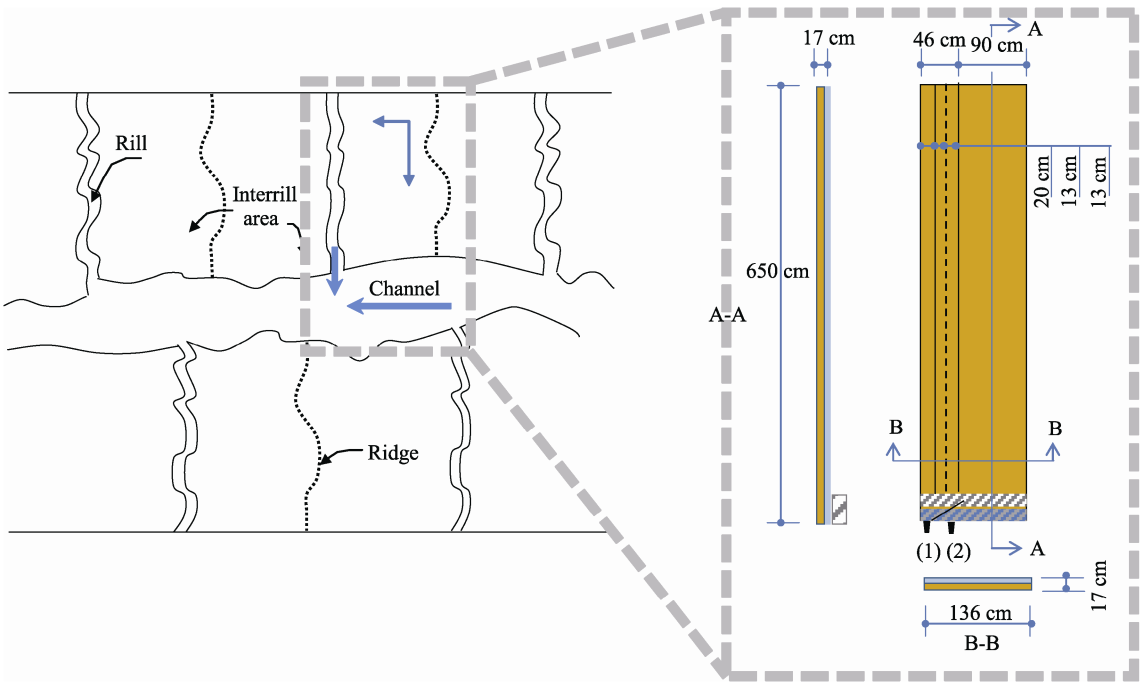

Fig. 2 Schematic description of microtopography in a watershed and plan view of the erosion flume (Aksoy et al., 2012)

portion of the interrill area is directed into the channel. By similarity principles, only one half of the channel, along with one rill and one interrill area, were modeled in the lab experiment. On the right side of Fig. 2, two outlets were formed on the flume. Outlet (1) is used for collecting flow from the rill while outlet (2) collects flow directly from the interrill area to the channel. Granting that the contribution of the flow to the channel coming directly from the interrill area is minor, measurement is still needed for mass conservation purposes in calibrating models.

Sand with a mean diameter of D_{50}=0.45 mm was used in the experiment. With noncohesive sand, enough transport capacity can be assured for erosion and sediment transport in the flume (Govers, 1990, 1992; Everaert, 1991; Abrahams et al., 1998; Ali et al., 2012). The particular size used represents medium sand as a representative size class.

The slope combination is 5% along the lateral and 10% along the longitudinal directions. The choice of slope combination was based on some studies done with field measurements. Chaplot and Le Bissonnais (2000) studied the influence of slope steepness (2% to 8%) on soil loss over interrill area. Thomaz and Vestena (2012) assessed the effect of different plot sizes on runoff and soil loss on an actual site with a hillslope degree of 7%. Hence, the choice of 5% along the lateral direction and 10% along the longitudinal direction of the hillslope is thought to be sufficient to induce erosion and sediment transport for this study.

Rainfall intensities of 45 and 105 mm/h were selected for this study to cover a wide range of rainfall intensities. The rainfall event with the intensity of 105 mm/h, which was applied first, was chosen as representative data for model calibration. For model validation, the event with the 45 mm/h rainfall intensity, which was applied later, was used. The duration of rainfall was 15 minutes for all experiments.

1.2 Mathematical formulation

1.2.1 Overland flow

For the overland flow model, the governing equations presented by Arguelles et al. (2013) have been used in the experimental setup to compute for the interrill and rill flow. Equation 1 for the interrill flow and Eq. 3 for the rill flow are given below:

$$\frac{\partial \bar{h}_o}{\partial t} + c\frac{\partial}{\partial x}\left(K_x \bar{h}_o^{\,3/2}\right) = \bar{q}_l - \left(\frac{\pi}{2}\right)^{3/2}\frac{K_y}{l}\bar{h}_o^{\,3/2}. \quad (1)$$

Where $\bar{h}_o$ is the width-averaged interrill flow depth (L);

$$c = \left(\frac{\pi}{2}\right)^{3/2}\left(\frac{1}{l}\right)\int_0^l \sin^{3/2}\left(\frac{\pi y}{2l}\right)dy = 1.09542, \quad (2a)$$

$$K_x = \frac{C_z S_{ox}^{3/2}}{\left[1+\left(\frac{S_{oy}}{S_{ox}}\right)^2\right]^{1/4}}, \quad (2b)$$

$$K_y = \frac{C_z S_{oy}^{3/2}}{\left[1+\left(\frac{S_{ox}}{S_{oy}}\right)^2\right]^{1/4}}. \quad (2c)$$

Where l is the interrill area width (L), C_z is Chezy's roughness coefficient ($L^{1/2}$/T), S_{ox} is the x-direction bed slope, S_{oy} is the bed slope in y-direction, and $\bar{q}_l$ is the width-averaged rainfall excess (L/T).

$$\frac{\partial h_r}{\partial t} + \frac{\partial}{\partial x}\left(K_r \frac{w_r^{1/2}h_r^{3/2}}{\left(w_r + 2h_r\right)^{1/2}}\right) = q_l + \left(\frac{\pi}{2}\right)^{3/2}\frac{K_y}{w_r}\bar{h}_o^{\,3/2}. \quad (3)$$

Where h_r is the rill flow depth (L), K_r=$C_{zr}S_{rx}^{1/2}$ (where, C_{zr} is Chezy's roughness coefficient for the rill ($L^{1/2}$/T), and S_{rx} is the bed slope in x-direction), w_r is the rill width (L), and q_l is the rainfall excess (L/T). Flow along the direction of the rill is defined by the x-coordinate while the y-coordinate is perpendicular to the direction of the flow along the rill.

Soil infiltration plays a significant role in runoff processes. In this study, Horton's infiltration model (Chow et al., 1988) was employed to describe the process of infiltration. It is expressed as:

$$f(t) = f_c + \left(f_0 - f_c\right)e^{-kt}. \quad (4)$$

Where f is the infiltration rate at time t (L/T), f_c is the terminal infiltration rate (L/T), f_0 is the initial infiltration rate (L/T), and k is a decay constant (/T). Rainfall excess rate is determined as the difference between rainfall intensity and infiltration rate.

1.2.2 Erosion and sediment transport

For the erosion-sediment transport model, the two-dimensional continuity equation of sediment can be given as:

$$\frac{\partial\left(hC_s\right)}{\partial t} + \frac{\partial\left(q_x C_s\right)}{\partial x} + \frac{\partial\left(q_y C_s\right)}{\partial y} = \frac{E}{\rho_s}. \quad (5)$$

Where h is overland flow depth (L), C_s is volumetric sediment concentration, t is time (T), x and y are axes of the coordinate system used in the scheme (L), q_x and q_y are discharges per unit width in the x- and y-directions ($L^{1/2}$/T), ρ_s is sediment density (M/L^3), and E is erosion (M/(L^2·T)) which is the sum of rainfall erosion (Wicks, 1988) and runoff erosion (Foster, 1982). The equation for erosion is given as:

$$E = \alpha R^{\beta} + \sigma\left(T_c - q_s\right). \quad (6)$$

Where the coefficient α is the soil detachability coefficient, R is the rainfall intensity (L/T), β is the exponent for rainfall impact erosion, σ is the transfer rate coefficient (/L), T_c is the transport capacity of flow (M/(L·T)), and q_s is the sediment discharge (M/(L·T)).

The one-dimensional form of mass conservation equation was derived from its two-dimensional form in Eq. 5 for a wide rectangular channel flow over interrill area by averaging over interrill area width using Chezy roughness equation together with kinematic wave approximation, as:

$$K_1 \frac{\partial}{\partial t}\left[\bar{h}(x;t)\overline{C_s}(x;t)\right] + K_2 \frac{\partial}{\partial x}\left[\left[\bar{h}(x;t)\right]^{3/2}\overline{C_s}(x;t)\right] = \frac{\bar{E}(x;t)}{\rho_s} - K_3\left[\left[\bar{h}(x;t)\right]^{3/2}\overline{C_s}(x;t)\right]. \quad (7)$$

Where

$$K_1 = \frac{\pi^2}{8}, \quad (8a)$$

$$K_2 = 0.4577\left(\frac{\pi}{2}\right)^{5/2} C_x S_{o,x}^{1/2}, \quad (8b)$$

$$K_3 = \left(\frac{\pi}{2}\right)^{5/2} \frac{1}{l_y} C_y S_{o,y}^{1/2}. \quad (8c)$$

A backward finite difference scheme (Strikwerda, 1989) was chosen to solve Eq. 7. Boundary and initial conditions were given as $\bar{C}_s(0,t)=0$ and $\bar{C}_s(x,0)=0$, respectively. In finite difference form, sediment concentration in the flow can be expressed as an explicit function of overland flow depth and sediment concentration at the current and previous time and space steps.

$$\bar{C}_s(x;t) = func\left\{\bar{h}(x;t-\Delta t), \bar{h}(x-\Delta x;t), \bar{h}(x;t), \bar{C}_s(x;t-\Delta t), \bar{C}_s(x-\Delta x;t)\right\}. \quad (9)$$

Parameters Δx and Δt in Eq. 9 are space and time increments, respectively. Overland flow depth is obtained from the hydrological part of the model whereas sediment concentration of the previous time and space steps are taken from the solution of the numerical algorithm for sediment transport equation.

Sediment eroded from interrill areas is transported by overland flow into rills where flow is concentrated. In this study, one-dimensional sediment continuity equation will be used together with Chezy roughness equation and kinematic wave approximation. For a rill carrying flow discharge, Q_R, through a rectangular cross-sectional area, A_R, the equation becomes:

$$\frac{\partial}{\partial t}\left[A_R(h_R)C_{s,R}\right] + \frac{\partial}{\partial x}\left[Q_R(h_R)C_{s,R}\right] = \frac{1}{\rho_s}(E_R + q_{s,IR}). \quad (10)$$

Where

$$A_R(h_R) = b_R h_R, \quad (11a)$$

$$Q_R(h_R) = C_R\sqrt{S_R}\left[\frac{(b_R h_R)^3}{b_R + 2h_R}\right]^{1/2}, \quad (11b)$$

$$E_R = \sigma(T_c - Q_{s,R}). \quad (11c)$$

Where E_R and $q_{s,IR}$ are erosion in the rill and lateral input coming from interrill areas, respectively. In Eq. 11, b_R is cross-sectional width of the rill, h_R is flow depth in the rill, C_R is the Chezy coefficient, S_R is slope of the channel, σ is the first order reaction coefficient for deposition (/L), T_c is flow transport capacity (M/T), and $Q_{s,R}$ is sediment load (M/T).

Lateral sediment load coming from interrill areas to the rill can be computed for unit width by:

$$q_{s,IR}(x,t) = \sum_{j=1}^{2} \rho_s C_{sj}(x,l_j;t) q_j(x,l_j;t). \quad (12)$$

Where j=1 and 2 refer to left and right side interrill areas of the rill, respectively. Using Eqs. 13 and 14,

$$\bar{h}(x;t) = \frac{\pi}{2} h(x,l_j;t), \quad (13)$$

$$\overline{C_s}(x;t) = \frac{\pi}{2} C_s(x,j;t). \quad (14)$$

Equation 12 can be further expressed as:

$$q_{s,IR}(x,t) = \left(\frac{\pi}{2}\right)^{5/2} \sum_{j=1}^{2} \rho_s \overline{C_s}_j(x,t) C_{yj} \bar{h}_j(x,t)^{3/2} S_{o,yj}{}^{1/2}. \quad (15)$$

It can be noted from Eq. 15 that lateral sediment input changes spatially along the rill and also with time. The same backward time and backward space finite difference was also used for the numerical solution of Eq. 10. Likewise, the same boundary and initial conditions used in interrill areas were also used and an explicit solution was obtained.

1.3 Performance measures

The coefficient of determination (R^2) and Nash-Sutcliffe Efficiency (NSE) were the statistical criteria used to evaluate model performance. Several studies (Krause et al., 2005; Moriasi et al., 2007; Mudgal et al., 2010) have quantified the values obtained by the statistical criteria. If the R^2 value is closer to 1, it means that observed and simulated values have strong correlation and values above 0.5 are considered acceptable. For NSE, if the value is near 1, it depicts an almost perfect fit. It has also been recommended that NSE greater than 0.5 be considered satisfactory and

NSE greater than 0.7 be considered good calibration.

2 Model calibration and validation

Trial and error method was employed in the calibration of parameters to give the best results for sediment load and yield.

For the interrill area, Aksoy and Kavvas (2001) identified α (soil detachability coefficient) and β (dimensionless exponent) for rainfall impact erosion, and σ (transfer rate coefficient or first order reaction coefficient for deposition), η (dimensionless coefficient) and ε (dimensionless exponent) for runoff erosion as the calibration parameters. For the rainfall impact erosion, the exponent β was fixed to either 1 or 2 and α remained to be the only parameter to be calibrated (Aksoy and Kavvas, 2001). In the simulation of the model, the initial values of β and α were set to 1. For the runoff erosion, it was observed that the most sensitive parameter during the calibration stage was η. Increasing the value of η also increased the peak of the sedigraph as expected since it is a factor for estimating the transport capacity, as indicated in $T_c=\eta(\tau-\tau_c)^{\varepsilon}$, where τ and τ_c are flow shear stress and its critical value, respectively.

For the rill erosion and sediment transport algorithm, model fitting is achieved by adjusting the first order reaction coefficient for deposition, σ_r. The other parameter being calibrated to attain satisfactory results is the dimensionless critical shear stress, τ_c. Both parameters have been observed to be sensitive such that slight changes in their values affect the resulting sedigraph.

With the use of the same values during the calibration stage, the model was validated against the sedigraph for the data set under the 45 mm/h rainfall intensity.

The erosion-sediment transport model produced good results for both calibration (Fig. 3; R^2=0.84, NSE=0.8) and validation (Fig. 4; R^2=0.83, NSE=0.72) runs based on the R^2 and NSE values. A summary of the initial and final parameter values after calibration of the model are shown in Table 1. In addition, scatter plots and cumulative mass curves are given in Figs. 5 and 6 and Figs. 7 and 8, respectively. These figures also suggest good correlation between measured and simulated values.

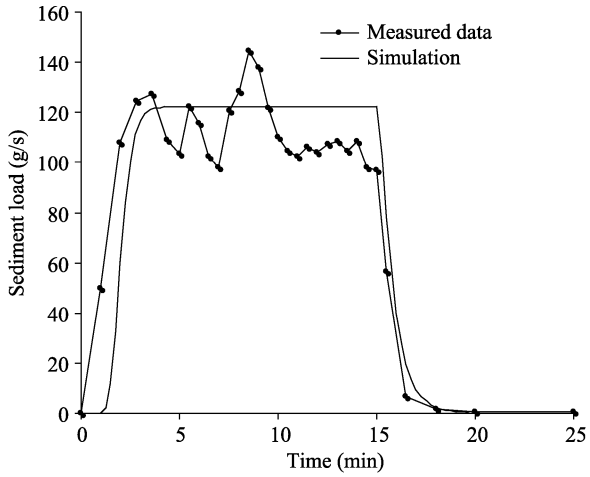

Fig. 3 Calibration of the erosion-sediment transport model for the combined rill and interrill areas with data set under the 105 mm/h rainfall intensity

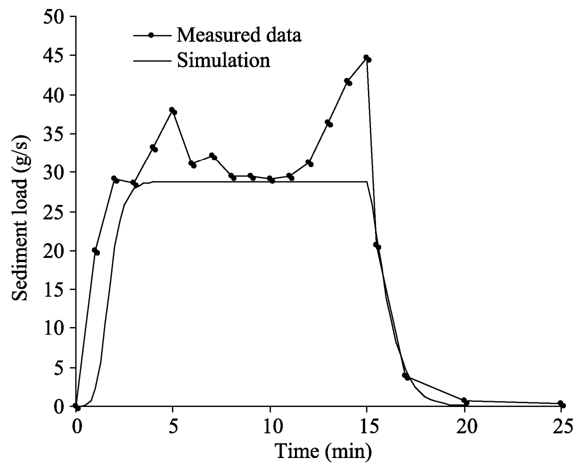

Fig. 4 Validation of the erosion-sediment transport model for the combined rill and interrill areas with data set under the 45 mm/h rainfall intensity

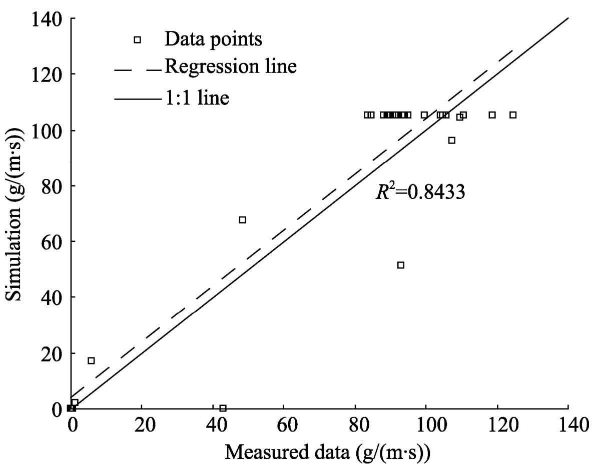

Fig. 5 Scatter plot of simulation vs. measured data for the calibration run

Table 1 Initial and final parameter values after calibration of the erosion-sediment transport model

Parameter	Interrill					Rill	
	σ (/m)	ε	η	β	α	σ_r (/m)	τ_c
Initial	1.00	1.00	0.050	1.00	1.00	0.051	0.060
Final	1.00	1.00	0.035	1.00	1.00	0.053	0.060

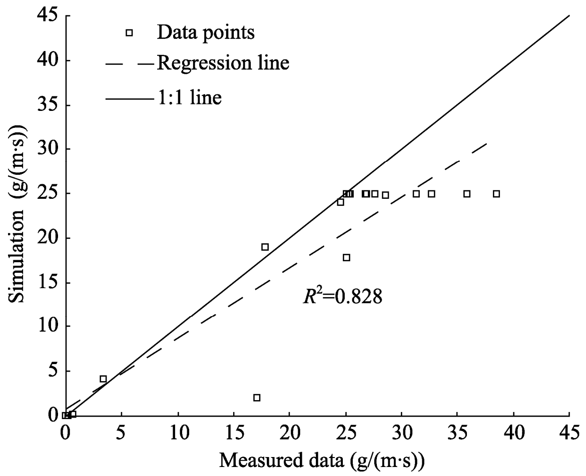

Fig. 6 Scatter plot of simulation vs. measured data for the validation run

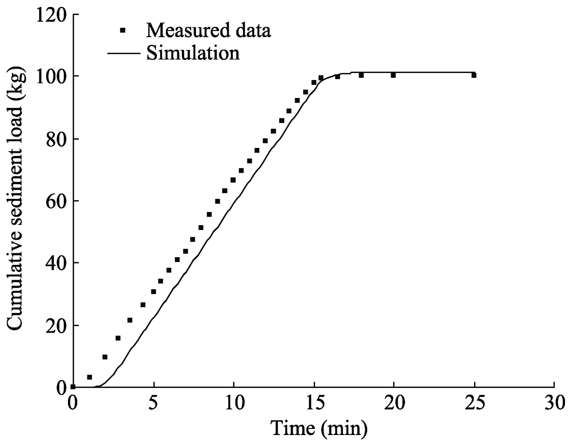

Fig. 7 Cumulative mass curve of simulated and measured data for the calibration run

3 Discussion

Simulation results in terms of sedigraph and cumulative mass curve were compared to the ones from other laboratory studies (Liu et al., 2006; Deng et al., 2008; An and Liu, 2009). In terms of sedigraph, immediate response from the plot, exhibited by the steep increase in the rising limb and followed by the equilibrium

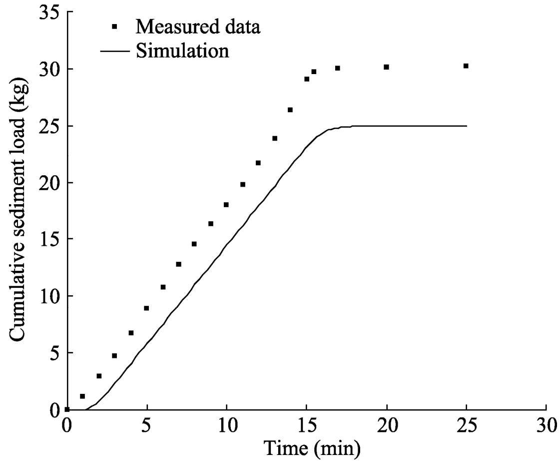

Fig. 8 Cumulative mass curve of simulated and measured data for the validation run

state and recession limb starting at the end of rainfall duration, was well depicted by the model and was compatible with the similar trend found in all the three studies (Liu et al., 2006; Deng et al., 2008; An and Liu, 2009). As for the cumulative sediment mass curve, more or less linear behavior of the curve was found after a brief initial period of slow increase. This also resembles the trend found in the above studies except for the work by An and Liu (2009) in which corresponding plot was not available. In general, both the observation and simulation results of this study are in good agreement with these laboratory flume studies in terms of their patterns.

The concept of spatial averaging used in this study allows the proposed model to deal better with the challenges that scale issues can bring as governing equations are scalable. Although the model's applicability has only been tested using laboratory data, the proposed model looks promising to perform well in the field conditions as, in the past, different models that share the similar construct of interrill and rill configuration had been used successfully in field conditions. Govindaraju and Kavvas (1991) applied the 1-D rill and interrill model and proved its field application. However, the model was limited by the inability to consider dynamic connection between rill and interrill. Tayfur (2001, 2007) later applied the 2-D and 0-D models and found that they also showed good applications. However, it was computationally more complicated in the case of 2-D, and in the case of the 0-D model, not enough details were provided along the hillslope length. From the successful applications of these models of similar construct, the proposed model in this study is expected to perform satisfactorily as it is of the same nature but at the same time can account for hillslope details.

Limitation of this study is that only sand soil was tested for the model. As such, further applicability of the model needs to be tested for different soil types. However, the majority of the flume studies have been performed using sand soil (Govers, 1990, 1992; Everaert, 1991; Abrahams et al., 1998; Ali et al., 2012) because of its wider applicability and availability. Also, the small number of data set used to test the model can bring an issue of uncertainty and be considered limitation of this study. However, in the few literatures (Liu et al., 2006; Deng et al., 2008; An and Liu, 2009) on hillslope erosion and sediment models based on laboratory experiments, two or three data sets were typically used for model testing. It is thought that the difficulty with rainfall simulation experiments and further analysis of water and soil samples made it difficult to obtain a sufficient number of data set. Nonetheless, it is acknowledged that more data would be desired for the testing of model applicability.

4 Conclusions

The goal of this study is to calibrate and verify the applicability of the physically based erosion-sediment transport model for two different rainfall intensities applied on an artificial erosion flume. The model-simulated results compared satisfactorily with the measured values as suggested by the calibration and validation statistics with R^2 values greater than 0.80 and NSE values greater than 0.70. With good statistical performance for both calibration and validation, the model is thought to be a useful and an important step towards verifying and improving the mathematical models of the process.

With the complexities involved in erosion and sediment transport processes, further validation of the model with data from more slope and rainfall combinations seems to be a desirable next step in strengthening the wide applicability of the model. In addition, application of the model to field data is also suggested to further test the model's capability.

Acknowledgements

This study was based on the international project "Development of a Hillslope-scale Sediment Transport Model" bilaterally supported by the National Research Foundation of Korea (NRF-2007-614-D00036, NRF-2008-614-D00018, NRF-2011-013-D00124 and NRF-2013R1A1A4A01007676) and TUBITAK (The Scientific and Technological Research Council of Turkey; 108Y250). This study was also supported in part by a grant (13CRTI-B052117-01) from the Regional Technology Innovation Program and another grant from the Advanced Water Management Research Program funded by the Ministry of Land, Infrastructure and Transport of the Korean Government, a 2011–2012 grant from Geum-River Environment Research Center, National Institute of Environmental Research, Korea, and a Korea University Grant.

References

Abrahams A D, Li G, Krishnan C, et al. 1998. Predicting sediment transport by interrill overland flow on rough surfaces. Earth Surface Processes and Landforms, 23: 1087–1099.

Aksoy H, Kavvas M L. 2001. A physically based erosion and sediment transport component for watershed hydrologic models. Hydrologic Research Laboratory, Department of Civil and Environmental Engineering, University of California, Davis, California.

Aksoy H, Erdem Unal N, Cokgor S, et al. 2012. A rainfall simulator for laboratory-scale assessment of rainfall-runoff-sediment transport processes over a two-dimensional flume. Catena, 98: 63–72.

Ali M, Sterk G, Seeger M, et al. 2012. Effect of hydraulic parameters on sediment transport capacity in overland flow over erodible beds. Hydrology and Earth System Sciences, 16: 591–601.

An Y, Liu Q Q. 2009. Two-dimensional hillslope scale soil erosion model. Journal of Hydrologic Engineering, 14: 690–697.

Arguelles A C C, Jung M, Pak G, et al. 2013. Evaluation of overland flow model for a hillslope using laboratory flume data. Water Science and Technology, 68(5): 1188–1194.

Chaplot V, Le Bissonnais Y. 2000. Field measurements of interrill erosion under different slopes and plot sizes. Earth Surface Processes and Landforms, 25: 145–153.

Chow V T, Maidment D R, Mays L W. 1988. Applied Hydrology. Singapore: McGraw-Hill Book Co., 109.

Deng Z Q, De Lima J L M P, Jung H S. 2008. Sediment transport rate-based model for rainfall-induced soil erosion. Catena, 76(1): 54–62.

Everaert W. 1991. Empirical relations for the sediment transport capacity of interrill flow. Earth Surface Processes and Landforms, 16: 513–532.

Foster G R. 1982. Modeling the erosion process. In: Haan C T, Johnson H P, Brakensiek D L. Hydrologic Modeling of Small Watersheds. St. Joseph, MI, USA: ASAE Monograph no. 5, 297–380.

Govers G. 1990. Empirical relationships on the transporting capacity of overland flow. In: Walling D E, Yair A, Berkowicz S. Erosion, Transport and Deposition Processes. Wallingford, UK: IAHS Publication, 45–63.

Govers G. 1992. Evaluation of transporting capacity formulae for overland flow. In: Overland Flow Hydraulics and Erosion Mechanics. London: University College London Press, 243–273.

Govindaraju R S, Kavvas M L. 1991. Modeling the erosion process over steep slopes: approximate analytical solutions. Journal of Hydrology, 127(1–4): 279–305.

Hirabayashi Y, Kanae S, Emori S, et al. 2008. Global projections of changing risks of floods and droughts in a changing climate. Hydrological Sciences Journal, 53(4): 754–772.

Krause P, Boyle D P, Base F. 2005. Comparison of different efficiency criteria for hydrological model assessment. Advances in Geosciences, 5: 89–97.

Liu Q Q, Xiang H, Singh V P. 2006. A simulation model for unified interrill erosion and rill erosion on hillslopes. Hydrological Processes, 20(3): 469–486.

Lopes V L. 1987. A numerical model of watershed erosion and sediment yield. PhD Dissertation. Tucson, AZ, USA: The University of Arizona.

Ma L, Wu J L, Abuduwaili J. 2011. The climatic and hydrological changes and environmental responses recorded in lake sediments of Xinjiang, China. Journal of Arid Land, 3(1), 1–8.

Mailhot A, Duchesne S. 2010. Design criteria of urban drainage infrastructures under climate change. Journal of Water Resources Planning and Management, 136(2): 201–208.

Morgan R P C, Quinton J N, Smith R E, et al. 1998. The European soil erosion model (EUROSEM): A dynamic approach for predicting sediment transport from fields and small catchments. Earth Surface Processes and Landforms, 23: 527–544.

Moriasi D N, Arnold J G, Van Liew M W, et al. 2007. Model evaluation guidelines for systematic quantification of accuracy in watershed simulations. Transactions of the ASABE, 50(3): 885–900.

Mudgal A, Baffaut C, Anderson S H, et al. 2010. Apex model assessment of variable landscapes on runoff and dissolved herbicides. Transactions of the ASABE, 53(4): 1047–1058.

Sharaiha R K, Ziadat F M. 2007. Alternative cropping systems to control soil erosion in arid to semi-arid areas of Jordan. African Crop Science Society, 8: 1559–1565.

Shaw H, Reisinger A, Larsen H, et al. 2005. Incorporating Climate Change Into Stormwater Design – Why and How? In: 4th South Pacific Conference on Stormwater and Aquatic Resource Protection. Auckland, New Zealand.

Smith R E. 1981. A kinematic model for surface mine sediment yield. Transactions of the ASABE, 24(6): 1508–1514.

Storm B, Jorgensen G H, Styczen M. 1987. Simulation of Water Flow and Soil Erosion Processes with a Distributed Physically-based Modeling System. Wallingford: IAHS Publications, 167: 595–608.

Strikwerda J C. 1989. Finite Difference Schemes and Partial Differential Equations. Pacific Grove, California: Wadsworth & Brooks.

Tayfur G. 2001. Modeling two-dimensional erosion process over infiltrating surfaces. Journal of Hydrologic Engineering, 6(3): 259–262.

Tayfur G. 2007. Modelling sediment transport from bare rilled hillslopes by areally averaged transport equations. Catena, 70(1): 25–38.

Thomaz E L, Vestena L R. 2012. Measurement of runoff and soil loss from two differently sized plots in a subtropical environment (Brazil). Earth Surface Processes and Landforms, 37: 363–373.

Toy T J, Foster G R, Renard K G. 2002. Soil Erosion: Processes, Prediction, Measurement, and Control. New York: John Wiley and Sons.

Wicks J M. 1988. Physically–based mathematical modelling of catchment sediment yield. PhD Dissertation. University of Newcastle upon Tyne.

Wicks J M, Bathurst J C. 1996. SHESED: A physically based, distributed erosion and sediment yield component for the SHE hydrological modelling system. Journal of Hydrology, 175: 213–238.